AIP | Journal of Applied Physics

Current-voltage characteristics and ON/OFF ratio in ferroelectric tunnel junctions

Xiaoyan Lu, Hui Li, and Wenwu Cao

Citation: J. Appl. Phys. **112**, 054102 (2012); doi: 10.1063/1.4748051
View online: http://dx.doi.org/10.1063/1.4748051
View Table of Contents: http://jap.aip.org/resource/1/JAPIAU/v112/i5
Published by the American Institute of Physics.

Current-voltage characteristics and ON/OFF ratio in ferroelectric tunnel junctions

Xiaoyan Lu,[1,2] Hui Li,[1,a)] and Wenwu Cao[2,a)]
[1]*School of Civil Engineering, Harbin Institute of Technology, Harbin 150001, China*
[2]*Materials Research Institute, The Pennsylvania State University, University Park, Pennsylvania 16802, USA*

(Received 12 April 2012; accepted 20 July 2012; published online 5 September 2012)

Current-voltage characteristics of poled ferroelectric tunnel junction have been theoretically studied with the consideration of piezoelectric effect and interface potential due to the depolarization effect. Compared with piezoelectric effect, barrier potential changed by polarization switching is more significant. Tunnel currents with low and high resistances during the reading process are distinct, which have potential applications as low-cost, high-density, and fast-speed ferroelectric memories. The obtained ON/OFF ratio in a symmetry $SrRuO_3/BaTiO_3/SrRuO_3$ structure is around 50 under a small applied voltage. © *2012 American Institute of Physics*. [http://dx.doi.org/10.1063/1.4748051]

I. INTRODUCTION

An electron can tunnel through a potential barrier higher than its energy with a finite probability if the barrier thickness is thin enough. The concept of tunneling came along with modern quantum mechanics, and soon after was used to explain a number of phenomena in 1930s, such as field emission and metal-vacuum-metal junctions.[1] Due to the progress in quantum theory and fabrication technologies, various junctions with barrier replaced by insulator or semiconductor, and metal replaced by superconductor, semiconductor, and ferromagnetic materials were investigated for vast applications. By far, non-polar dielectric materials have been commonly used as barriers. Although a polar barrier was proposed to form a ferroelectric tunnel junction as early as 1971 by Esaki *et al.*,[2] experimental investigations on ferroelectric tunnel junctions (FTJs) only began in recent years due to the tremendous improvement in nano scale fabrication and characterization techniques.[3–9] Heterostructures composted of ferroelectric ultrathin layer sandwiched between oxide electrodes were prepared to gain large tunnel junction resistance by switching the polarization. However, only small ON/OFF ratio was reported.[2,10,11] Recently, a large ON/OFF ratio of 100 was reported in an array of normal ferroelectric junctions. Researchers used a large pulse voltage to write the junctions into different polarization states as reference states, then read them by using a conductive-tip atomic force microscopy with small voltage.[5,6] Compared with non-polar barrier, ferroelectric tunnel junction with electric controllable polarized barrier is fast, low-cost to write, and easy to read. With the interplay among ferroelectricity, ferromagnetism and electron tunneling, more fascinating multi-state memories, such as multiferroic tunnel junctions, can be expected in the near future.[12–16]

To gain large resistance change, tunneling current may be controlled by external electric field using ON and OFF states. According to Simmons,[17] tunneling current depends exponentially on the barrier thickness, square root of the effective electron mass and square root of barrier potential height. Therefore, even a small change in any of these parameters may have a considerable effect on the tunneling current.[9] For a ferroelectric tunnel junction, the effective thickness, effective electron mass, and barrier conduction-band edge can be changed with the application of an electric field due to the piezoelectric effect. Besides, since electrons can exist within a typical Tomas-Fermi screening length in non-ideal electrodes, depolarization field induced by incompletely screened bound charges can significantly change the average barrier height.[18] With the low and high barrier potentials in the polarization up and down states, the tunneling currents can be recognized as ON and OFF states during the reading process. As shown below, this effect is much greater than the piezoelectric effect and could be regarded as the main origin of high and low tunneling resistance states.

To be an electric switchable barrier, the ferroelectric thin film should be thick enough to maintain the ferroelectric property, and on the other hand, thin enough to act as a barrier with finite tunneling probability. Both experimental and theoretical works have proven that the critical thickness of ferroelectric layer under large compressive strain can be down to one to two nanometers, which guarantees the tunneling possibility.[19–22] However, we should keep in mind that the ferroelectric could be in metastable state, and the dielectric and piezoelectric response could be great but with high sensitivity to environmental changes since the thickness is very close to the critical thickness. We will study these properties for poled ferroelectric films, the poled states with up and down polarizations will be severed as the fundamental states in the reading process. Barrier potentials induced by the depolarization field with different polarization states will be calculated. Then, current-voltage characteristics of junctions with different polarization states will be analyzed and compared. The modification of tunneling current by the piezoelectric effect is also studied.

II. THEORETICAL MODEL

A specialized FTJ composted of two symmetric conducting $SrRuO_3$ electrodes separated by an ultrathin $BaTiO_3$

a)Authors to whom correspondence should be addressed. Electronic addresses: lihui@hit.edu.cn and dzk@psu.edu.

layer in a junction array is illustrated in Fig. 1. The axis was set at the interface of the bottom electrode and the barrier. The thickness of electrodes and barrier are l_e and l, respectively. $NdGaO_3$ was chosen as the substrate due to the large achievable external strain of -3.2%.[4] In the writing process, high positive and negative pulse electric fields were applied by using piezoresponse force microscope (PFM) to gain polarization up and down states in each junction elements. In the reading process, tunnel currents were read by a conductive-tip atomic force microscope (CTAFM).

A. Writing process

Since the poled FTJ elements are the fundamental state for information storage and also serve as the reference for the following reading process, we first use a modified phenomenological theory to predict the ferroelectric, dielectric, and piezoelectric properties of the poled ultrathin ferroelectric film.[23] The depolarization field, which is responsible for the interface potential for electron tunneling, was derived from the electric balance condition in the system.

With sufficient substrate strain, the polarization can be stabilized in the direction perpendicular to the film surface. The electric displacement along the film normal direction can be expressed as $D = \varepsilon_0 E + P_I + P = \varepsilon_b E + P$,[24] where ε_0 is the vacuum dielectric permittivity; E is the electric field; $P_I = \chi_I E$ is the linear part of the induced polarization, which is usually very small but commonly exists in dielectric materials with a value proportional to the linear field-dependent electric susceptibility χ_I; $\varepsilon_b = \varepsilon_0 + \chi_I$ is the dielectric permittivity of the background material.[25] ε_b was reported to vary with thickness and temperature.[26] However, we follow the convention to assume it as a constant.[25] It should be noted that this value has significant effect on the predicted results; therefore, more rigorous considerations are still needed. The polarization P is chosen as the order parameter. The corresponding dielectric permittivity is nonlinear and may vary with the film thickness, temperature, and boundary conditions. The equilibrium of the system under an electrostatic field E can be derived by minimizing the Gibbs free energy, treating D as a linear function of E[23]

$$g = f(P)|_{E=0} - \frac{1}{2}E^2 - PE, \tag{1}$$

where the first term is the corresponding free energy under zero electric field.

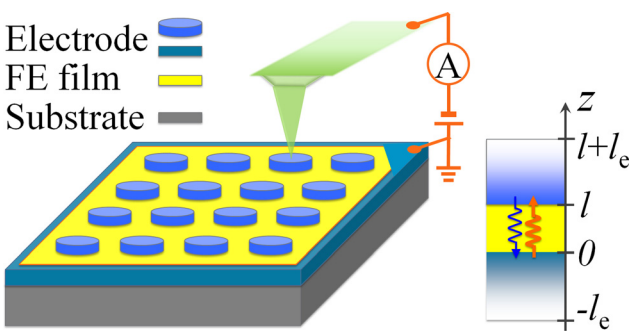

FIG. 1. Schematic illustration of a ferroelectric tunnel junction array and the calculation model.

Since the film is under a constant substrate strain, it should be considered as a Helmholtz free energy and can be expressed as $f(P)|_{E=0} = f(P)|_{\sigma=0} + f_{Ela}$[27] with the free energy density of unstrained film $f(P)|_{\sigma=0}$ plus the elastic energy density $f_{Ela} = \bar{G}(u_m - Q_{12}P^2)^2$. Here, σ is the stress vector, $\bar{G} = C_{11} + C_{12} - 2C_{12}^2/C_{11}$ is the effective elastic modulus, C_{ij} are the elastic stiffness coefficients, and Q_{12} is the electrostrictive coefficient.

With the contributions of elastic energy, surface energy, and electrostatic energy, the total free energy expanded in terms of the order parameter P can be rewritten as[22–25]

$$F = \left(\frac{\alpha^*}{2}P^2 + \frac{\beta^*}{4}P^4 + \frac{\gamma}{6}P^6 + \bar{G}u_m^2 - \frac{1}{2}\varepsilon_b E^2 - PE\right)l + F_S, \tag{2}$$

where $\alpha^* = \alpha_0(T - T_{c0}) - 4Q_{12}u_m\bar{G}, \beta^* = \beta + 4Q_{12}^2\bar{G}$ are the renormalized coefficients with the consideration of substrate strain, α_0, β, and γ are the expansion coefficients of the Landau free energy, T is the temperature, T_{c0} is the Curie temperature of the counterpart bulk material, and F_S is the surface energy. Since the film is ultrathin, the effective surface energy can be assumed as uniform and written as a Taylor series expansion. By keeping the two lowest order terms, it can be expressed as $F_S = (\xi_{11} - \xi_{12})P + (\xi_{21} + \xi_{22})P^2/2$, where ξ_{11}, ξ_{12} and ξ_{21}, ξ_{22} are expansion coefficients of the two surfaces, respectively,[22] For a symmetric structure, the surface energy can be simplified as $F_S = \xi P^2$. The electrostatic field E is the total electric field on the barrier, i.e., the effective external electric field E_{eff} plus the depolarization field E_d induced by the incomplete screening effect.

The depolarization field can be quite strong and may partially suppress the polarization, especially when the film is very thin. Assuming the polarization induced compensation charges in the metal electrodes are $\pm q_e$, under boundary conditions of $E_{ele}(z) = 0$ at the outer surface of the electrode and $E_{ele}(z) = q_e/\varepsilon_e$ at the interface of the film/electrode, the electric field in the bottom electrode can be solved from the Poisson's equation as[17]

$$E_{ele}(z) = \frac{q_e}{\varepsilon_e}\frac{\sinh[(l_e + z)/l_s)]}{\sinh(l_e/l_s)}, \tag{3}$$

where ε_e is the dielectric constant of the electrode and l_s is the screening length that characterizes the free charge distribution within the electrode. Under external voltage V on the outer surfaces of the electrodes, the final static electric balance condition can be written as

$$2\int_{l_e} E_{ele}\,dz + \int_{l} E_{film}\,dz = V, \tag{4}$$

where E_{film} is the total electric field in the film. By using the displacement continuity in the interface $D_{film} = \varepsilon_b E_{film} + P = q_e$, the total electric field can be expressed as $E_{film} = (q_e - P)/\varepsilon_b$. Submitting it into Eq. (4), one can derive the induced compensation charges q_e as

$$q_e = (P + V\varepsilon_b/l)\theta \tag{5}$$

with $\theta = \frac{l}{\varepsilon_b}/\left(\frac{2l_s}{\varepsilon_e} + \frac{l}{\varepsilon_b}\right)$. The total effective electric field in the film can then be derived as

$$E_{\text{film}} = \frac{-P(1-\theta)}{\varepsilon_b} + \frac{V}{l}\theta = E_d + E_{\text{eff}}. \quad (6)$$

The first term is the depolarization field E_d and the second term is the effective electric field E_{eff} in the film. Because a potential drop exists in the electrodes, the effective voltage applied onto the barrier depends on the ratio of film thickness to the screening length of the electrodes. Obviously, if there is no external applied voltage, the internal electric field is just the depolarization field, i.e., $E_{\text{film}} = E_d$.[17,24] If the film is thick enough or electrodes are perfect, corresponding to $\theta = 1$ or $l_s = 0$, no depolarization field exists in short circuit condition, and the internal electric field will be the simple form of V/l. However, when the film is ultrathin with imperfect conductor electrodes, both the depolarization field and the effective electric field in the film will be affected by those trapped charges in the electrodes, which will highly impact on the performance of the polarization and interface potential under an external electric field.

Under a total internal electric field $E_d + E_{\text{eff}}$ in the barrier, the time-evolution of the polarization in the barrier is proportional to the variation of the total free energy in Eq. (2) with respect to the polarization

$$\frac{\partial P}{\partial t} = -M\frac{\delta F}{\delta P} = -Ml(\alpha^{**}P + \beta^* P^3 + \gamma P^5 - E'_{\text{eff}}), \quad (7)$$

where $\alpha^{**} = \alpha^* + (1-\theta^2)\varepsilon_b^{-1} + 2\xi l^{-1}$ is the renormalized coefficient, M is the kinetic coefficient, and the last term $E'_{\text{eff}} = \theta^2 V/l = \theta E_{\text{eff}}$ is the nominal electric field with the consideration of depolarization effect.

Piezoelectric strain was believed to have significant effect on the tunneling current.[9] In linear approximation, piezoelectric strain can be expressed as $\Delta S = d^*_{33}E_{\text{eff}}$, d^*_{33} is the effective piezoelectric coefficient for constrained film under a small applied electric field. Considering uniform in-plane strain $S_1 = S_2 = u_m$ and vertical stress free ($T_3 = 0$), the piezoelectric coefficient can be expressed by the derivative of the vertical total strain S_3 with respect to the effective electric field applied on the film:[28]

$$d^*_{33} = \frac{dS_3}{dE_{\text{eff}}} = 2\bar{Q}(P+P_I)\frac{\partial(P_I+P)}{\partial E_{\text{eff}}}\bigg|_{V\approx 0} = 2\bar{Q}(P+\chi_I E_{\text{film}})(\chi^*_I + \theta\chi_S), \quad (8)$$

where $S_3 = \bar{s}u_m + \bar{Q}(P_E+P)^2$; $\bar{s} = 2s_{12}(s_{11}+s_{12})^{-1}$ and $\bar{Q} = Q_{11} - \bar{s}Q_{12}$ are the effective elastic compliance and electrostrictive coefficient, respectively; $\chi^*_I = \partial P_I/\partial E_{\text{eff}} = \partial\chi_I E_{\text{film}}/\partial E_{\text{eff}} = \chi_I(1 - \frac{1-\theta}{\varepsilon_b}\theta\chi_S)$, where χ_S is the spontaneous susceptibility $\chi_S = \partial P/\partial E'_{\text{eff}} = (\alpha^{**} + 3\beta^* P^2 + 5\gamma P^4)^{-1}$. Usually, χ_S is much larger than χ_I, especially near the critical point. However, χ_I cannot be ignored when the film is very thin or when the spontaneous susceptibility is very small with non-zero electric field. Without applied field, the effective piezoelectric coefficient can be approximated as $d^*_{33} = 2\bar{Q}P\theta\chi_S$. It is size dependent and generally different from that of thicker films.[27]

B. Reading process

Tunneling current through a barrier describes the difference of the forward and backward currents between the two electrodes. If the electrodes are equipotential, the system is in thermodynamic equilibrium and the Fermi levels of electrodes coincide; hence, there is no current. For poled ferroelectric tunnel junction under short circuit condition, asymmetric potential exist on the two interfaces of the barrier/electrode due to the depolarization field as described above. However, without application of external electric field, there is still no current because the outer sides of the electrodes are in the same potential, and the electrostatic relation is strong enough to forbid electron tunneling under normal condition. However, the shape of the asymmetric potential, which is dependent on the direction of the polarization, can significantly change the average barrier potentials; thus, the currents with ON and OFF states can be read by a small voltage.

Following Simmons' method, the tunneling current can be calculated by using the Fermi-Dirac statistics and the penetration probability of electrons calculated based on the WKB approximation. Assuming the mass of electrons m is isotropic in space, the penetration probability for an electron with kinetic energy of $E_z^{(e)}$ in the film normal direction through a barrier potential of $U(z)$ of arbitrary shape can be expressed as[16]

$$D(E_z^{(e)}) = \exp\left[-\frac{2}{\hbar}\int_s \sqrt{2m(U(z)-E_z^{(e)})}dz\right]. \quad (9)$$

Assuming the tunneling probability for electrons in different directions are the same, under an applied voltage V, the net flow of electrons N through the barrier is given by

$$N = \frac{m}{2\pi^2\hbar^3}\int_0^{E_\infty^{(e)}} D(E_z^{(e)})dE_z^{(e)}\int_0^\infty [f(E^{(e)}) - f(E^{(e)}+eV)]dE_r^{(e)}, \quad (10)$$

where $\hbar$ is the Planck's constant; e is the electron charge; and $f(E^{(e)})$ is the Fermi-Dirac distribution function $f(E^{(e)}) = \left[1 + \frac{\exp(E^{(e)}-\eta)}{k_B T}\right]^{-1}$, where η is the Fermi level of the electrode and k_B is the Boltzmann constant. For the convenience of integration of Eq. (10), the total energy of a single electron, $E^{(e)}$, can be expressed in the polar coordinates as $E^{(e)} = E_z^{(e)} + E_r^{(e)}$ and $E_r^{(e)} = E_x^{(e)} + E_y^{(e)}$.

To simplify the integral, we assume $T = 0$ and use the rectangular potential barrier proposed by Simmons. The current density $J = Ne$ can be written as[16]

$$J = \frac{me}{2\pi^2\hbar^3}\left[eV\int_0^{\eta-eV}\exp\left(-\Lambda\sqrt{\eta+\bar{\varphi}-E_z^{(e)}}\right)dE_z^{(e)} + \int_{\eta-eV}^{\eta}\left(\eta - E_z^{(e)}\right)\exp\left(-\Lambda\sqrt{\eta+\bar{\varphi}-E_z^{(e)}}\right)dE_z^{(e)}\right] \quad (11)$$

with $\Lambda = 2l\sqrt{2m}/\hbar$, which has the dimension of $J^{-1/2}$, $\bar{\varphi}$ is the average barrier height with reference to the Fermi level. Integrating Eqs. (12a)–(12c), the current per meter square can be expressed as $J = \frac{1}{2}me\pi^{-2}\hbar^{-3}(j_1 + j_2 + j_3)$ with

$$j_1 = \left[\frac{4\bar{\varphi}}{\Lambda^2} + \frac{12}{\Lambda^4}(\Lambda\sqrt{\bar{\varphi}} + 1)\right]\exp(-\Lambda\sqrt{\bar{\varphi}}), \quad (12a)$$

$$j_2 = -\left[\frac{4(\bar{\varphi}+eV)}{\Lambda^2} + \frac{12}{\Lambda^4}\left(\Lambda\sqrt{\bar{\varphi}+eV}+1\right)\right]\exp\left(-\Lambda\sqrt{\bar{\varphi}+eV}\right), \quad (12b)$$

$$j_3 = -\frac{2eV}{\Lambda^2}(\Lambda\sqrt{\eta+\bar{\varphi}}+1)\exp(-\Lambda\sqrt{\eta+\bar{\varphi}}), \quad (12c)$$

Actually, Λ is an indirect functional of V because of the converse piezoelectric strain effect on the effective barrier thickness, electron mass, and barrier conduction-band edge. To simplify our calculations, we transform this parameter out of the integral. V is the effective voltage on the film with the consideration of the size effect and depolarization influence. The last term j_3 is usually very small because the Fermi level is much higher than the applied voltage potential. We also note that Simmons ignored the second term in j_1 and j_2 because of the lower order in terms of Λ. In our calculations, these terms appear to have considerable influence, hence, cannot be ignored.

Piezoelectric strain ΔS induced by the application of an electric field along the thickness direction of the film is linearly proportional to the piezoelectric coefficient $\Delta S = d_{33}^* E_{\text{eff}}$. With piezoelectric effect, the effective thickness, effective electron mass, and the barrier conduction-band edge are modified to $l^* = l(\Delta S + 1)$, $m^* = m(1 + \mu_{33}\Delta S)$, and $\varphi_c = \varphi_c^0 + \kappa_3\Delta S$, respectively; l, m, and φ_c^0 are the barrier length, electron mass, and barrier conduction-band edge above the Fermi level at $V = 0$, respectively; μ_{33} is the coefficient describing the change of mass with respect to strain; κ_3 is the relevant deformation potential of the conduction band under strain.[9] We note that if we use $m^* = m_0(1 + \mu_{33}\Delta S)$ with m_0 to be the effective electron mass with value of $0.2\,m$ at $V = 0$,[9] the current will be overestimated by about two orders of magnitude than the experimental results. More attention should be paid to the effective electron mass. With the up and down polarization states, the initial average barrier potential is $\bar{\varphi}^0 = \varphi_c^0 + \kappa_3\Delta S \mp E_d l^* e/2$. Since the applied voltage is comparable with but smaller than the average barrier potential, it is in an intermediate-voltage range as given in Ref. 17. When an voltage is applied to read the junction, the average potential becomes $\bar{\varphi} = \bar{\varphi}^0 + Ve/2$. The current now becomes $J = \frac{1}{2}m^* e\pi^{-2}\hbar^{-3}(j_1 + j_2 + j_3)$ with modified $\bar{\varphi}$ and $\Lambda^* = 2l^*\sqrt{2m^*}/\hbar$.

III. RESULTS AND DISCUSSIONS

A. Ferroelectric and piezoelectric properties

The parameters (listed in Table I) used for $BaTiO_3$ and electrode $SrRuO_3$ were taken from Refs. 19 and 24. The calculations for the properties of $BaTiO_3$ were carried out at room temperature. The Dirac-Fermi distribution function was taken at $T = 0\,K$ for simplicity.

Since large compressive strain can counterbalance the detrimental influence of size reduction and preserve ferroelectricity at very low thickness, strain engineering is a key to make switchable high quality ultrathin ferroelectric films. Spontaneous polarization under various substrate misfits are shown in Fig. 2. Under a strain of -3.2%, the critical temperature is above 500 K for a film with a thickness of 2 nm. Even under a smaller external compressive strain of -2.8%, the critical temperature is still above room temperature for a 2 nm film. Low critical thickness at room temperature is necessary for FTJs with ferroelectric barrier. The critical thickness estimated from the insert of Fig. 1 is 1.5 nm for the film under a strain of -3.2%, and 1.9 nm for the film under a strain of -2.8%. Under an applied ac voltage with a frequency of 1 kHz, the $BaTiO_3$ film with the thickness of 2 nm and a misfit compressive strain of -3.2% exhibits a good hysteresis loop (insert in Fig. 2). However, it is important to keep in mind that the properties of the ultrathin film might be less stable since the thickness is quite close to the critical thickness.

TABLE I. Parameters of the $BaTiO_3$ and $SrRuO_3$.

$BaTiO_3$	$\alpha = 6.6 \times (T - 383) \times 10^5\ C^{-2}m^2N$, $\beta = -14.4 \times 10^6(T - 448.15)\ C^{-4}m^6N$, $\gamma = 39.6 \times 10^9\ C^{-6}m^{10}N$, $Q_{11} = 0.11\ C^{-2}m^4$, $Q_{12} = -0.043\ C^{-2}m^4$, $s_{11} = 8.3 \times 10^{-12}\ m^2N^{-1}$, $s_{12} = -2.7 \times 10^{-12}\ m^2N^{-1}$, $s_{13} = -2.7 \times 10^{-12}\ m^2N^{-1}$, $\varepsilon_b = 90\,\varepsilon_0$; $\varphi_c^0 = 0.5$ eV, $\kappa_3 = -4.5$ eV, and $\mu_{33} = 10$, $m_0 = m_e$.
$SrRuO_3$	$\varepsilon_{e1} = \varepsilon_{e2} \approx 8.45\,\varepsilon_0$, $\varepsilon_0\xi \approx 0.01 \times 10^{-10}$ m, $l_{s1} = l_{s2} \approx 0.6 \times 10^{-10}$ m; $m_e = 9.1094 \times 10^{-31}$ kg, $\varepsilon_0 = 8.85 \times 10^{-12}$ F/m.

Polarization, dielectric, and piezoelectric properties vs. voltage is shown in Fig. 3. The magnitude of polarization P has a slight increase under the application of an electric field compared with the one without field. The nonlinear relationship of the polarization vs. voltage illustrates the nonlinear dielectric response. The susceptibility χ_S decreases sharply from an initial relatively high normalized value of about 170 to about 16 under high voltage. Due to the dielectric singularity at the critical point, large dielectric coefficient can exist in the vicinity of the critical thickness.[29] Since the piezoelectric coefficient is related to the dielectric coefficient, an enhancement of the piezoelectric coefficient is also expected.[30] Although piezoelectric coefficient was reported

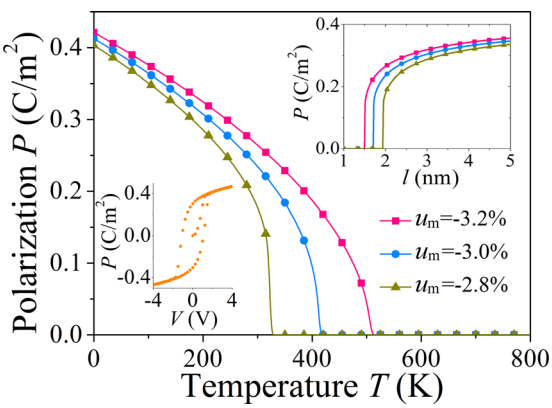

FIG. 2. Temperature-dependent of polarization showing transition from high temperature to low temperature phases. Misfit strains of -3.2%, -3.0%, and -2.8% are given for comparison. Inserts are room temperature hysteresis loop, and thickness-dependent polarization under different misfit strains.

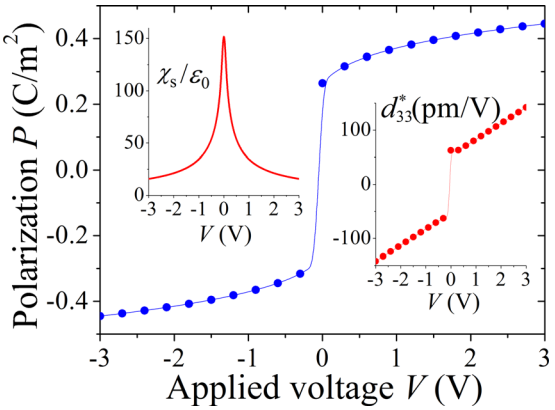

FIG. 3. Polarization vs. voltage for a film with the thickness of 2 nm under a misfit strain of −3.2% at $T = 300$ K. Inserts are the behaviors of normalized susceptibility and piezoelectric response.

to vary from 2–5 pm/V for ultrathin film to 95 pm/V for the bulk-like film,[4] the effective piezoelectric coefficient for poled film with the thickness of 2 nm was calculated to be about 55 pm/V under zero field and increases with applied electric field (insert of Fig. 3). This is opposite to the field effect in thick films for which the piezoelectric coefficient decreases with electric field.[27] This difference was mainly attributed to the large electric-induced polarization and linear field-dependent susceptibility, which are very small in thick films.

B. Current-voltage characteristics

As stated above, the initial up and down polarization states are responsible for the low and high barrier height, and the ON and OFF current states under small reading voltage. Before comparing the currents of the two states, we first studied the influence of piezoelectric and depolarization effects on the effective barrier thickness, electron mass, and

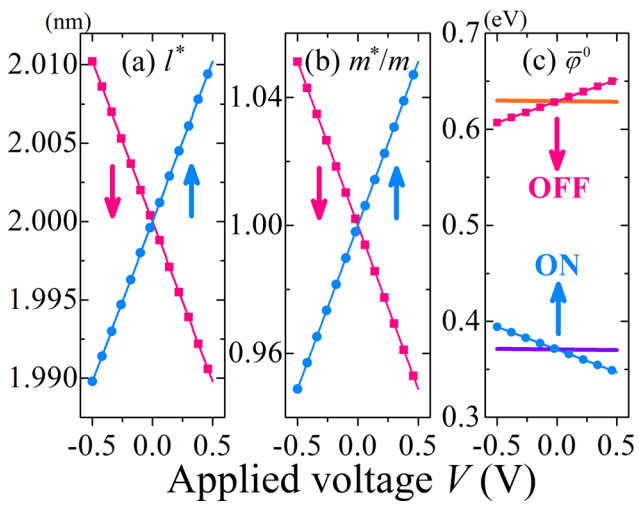

FIG. 4. (a) Effective barrier thickness and (b) effective electron mass with the consideration of piezoelectric effect in film with different polarization. (c) Low and high barrier potentials with P up and down, respectively. Barrier potentials without modification of piezoelectric strain on the conductance are displayed as solid lines in (c) for comparison. (Pink: polarization down corresponds to high resistance state; blue: polarization up corresponds to low resistance state).

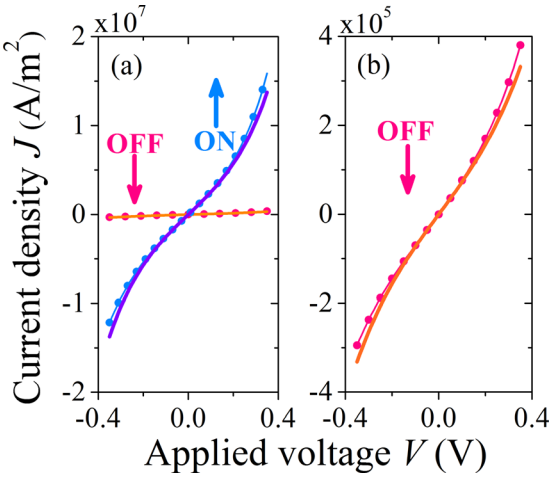

FIG. 5. (a) Current-voltage characteristics of low and high resistances. (b) Current-voltage characteristics of high resistance for a separated review. With (line with solid circles) and without (solid line) piezoelectric effect are provided for comparison.

conduction-band edge. As shown in Fig. 4, under the applied voltage between −0.5 and 0.5 V, the effective barrier thickness is changed from 1.99 nm to 2.01 nm for a film with thickness of 2 nm, about 1%, and the change of the electron mass is about 2%. Although the tunneling current is exponentially dependent on the thickness and the square root of the effective electron mass, these piezoelectric induced changes are too small compared with the polarization-switching induced barrier potential change. The average barrier potential is only modified slightly by the piezoelectric effect (solid line in Fig. 4(c)). On the contrary, the change given by the depolarization is quite noticeable during the polarization switching. As shown in Fig. 4(c), with an average absolute depolarization-field induced potential ($eE_d l^*/2$) of about 0.13 eV, the average high and low barrier potentials, which correspond to a polarization of up and down states, are about 0.63 eV and 0.37 eV, respectively, which is the key for the high and low resistance states.

The current-voltage characteristics in a symmetric FTJ at 300 K are shown in Fig. 5. The ON and OFF states, i.e., low and high resistance state with the high and low current densities, correspond to the positive and negative polarizations, respectively. The current densities of low-resistance and high-resistance states in this symmetry structure are on the order of 10^7A/m^2 and 10^5A/m^2, respectively. There are no experimental results for the symmetric FTJ structures, but experimental values for the current densities of low-resistance and high-resistance states of an asymmetric structure are about 1.6×10^8A/m^2 and 1.6×10^6A/m^2, respectively.[3] The difference between the theoretical and experimental values may be caused by the additional change of barrier potential induced by the built-in field in an asymmetry structure.

IV. CONCLUSIONS

Tunneling currents across a symmetry ferroelectric tunnel junction were theoretically studied with the consideration of polarization switching, piezoelectric effect, and interface potential due to the depolarization effect. Although the

ferroelectric properties of ultrathin ferroelectric barrier were predicted to be comparable with those of thick film counterpart with the assistance of large substrate strain and oxide electrodes, the piezoelectric effect on the tunnel current is still much weaker than the modification of the barrier potential by the polarization switching. The change of the barrier potential can also be enhanced by the substrate stain or by asymmetric structure with designed electrodes. Even in this non-optimized symmetric FTJ structure, the magnitude of the low-resistance current is still about 50 times higher than that of the high-resistance state, presenting a clear distinction between the ON and OFF states. Further structural optimization may be through the design of asymmetric FTJ structures with designed electrodes to give even larger stable ON and OFF ratios.

ACKNOWLEDGMENTS

We thank Professor Earle Ryba and Professor Wenhua Jiang (Materials Research Institute, Pennsylvania State University) for valuable discussions. This research was supported by the Ministry of Science and Technology (No. 2011BAK02B02), National Science Foundation of China (Nos. 11002044, 51078107), the China Postdoctoral Science Foundation (Nos. 20090460068, 201104437), and the Oversea Study Program from the Harbin Institute of Technology.

[1]L. Solymar, *Superconductive Tunnelling and Applications* (Wiley, New York, 1972).
[2]L. Esaki, R. Laibowitz, and P. Stiles, IBM Tech. Discl. Bull. **13**, 2161 (1971).
[3]J. Rodriguez-Contreras, H. Kohlstedt, U. Poppe, R. Waser, C. Buchal, and N. Pertsev, Appl. Phys. Lett. **83**(22), 4595 (2003).
[4]A. M. Ionescu, Nat. Nanotechnol. **7**(2), 83 (2012).
[5]V. Garcia, S. Fusil, K. Bouzehouane, S. Enouz-Vedrenne, N. D. Mathur, A. Barthelemy, and M. Bibes, Nature (London) **460**(7251), 81 (2009).
[6]A. Chanthbouala, A. Crassous, V. Garcia, K. Bouzehouane, S. Fusil, X. Moya, J. Allibe, B. Dlubak, J. Grollier, and S. Xavier, Nat. Nanotechnol. **7**, 101 (2011).
[7]A. Gruverman, D. Wu, H. Lu, Y. Wang, H. Jang, C. Folkman, M. Y. Zhuravlev, D. Felker, M. Rzchowski, and C. B. Eom, Nano Lett. **9**(10), 3539 (2009).
[8]D. Pantel, S. Goetze, D. Hesse, and M. Alexe, ACS Nano **5**(7), 6032 (2011).
[9]D. I. Bilc, F. D. Novaes, J. Íniguez, P. Ordejón, and P. Ghosez, Acs Nano **6**(2), 1473 (2012).
[10]H. Kohlstedt, N. A. Pertsev, J. R. Contreras, and R. Waser, Phys. Rev. B **72**(12), 125341 (2005).
[11]M. Y. Zhuravlev, R. F. Sabirianov, S. Jaswal, and E. Y. Tsymbal, Phys. Rev. Lett. **94**(24), 246802 (2005).
[12]J. Scott, Nature Mater. **6**(4), 256 (2007).
[13]M. Gajek, M. Bibes, S. Fusil, K. Bouzehouane, J. Fontcuberta, A. Barthélémy, and A. Fert, Nature Mater. **6**(4), 296 (2007).
[14]J. D. Burton, and E. Y. Tsymbal, Phys. Rev. Lett. **106**(15), 157203 (2011).
[15]Y. Zheng and C. Woo, Nanotechnology **20**, 075401 (2009).
[16]E. Tsymbal, A. Gruverman, V. Garcia, M. Bibes, and A. Barthélémy, MRS Bull. **37**(02), 138 (2012).
[17]J. Simmons, J. Appl. Phys. **34**, 1793 (1963).
[18]R. Mehta, B. Silverman, and J. Jacobs, J. Appl. Phys. **44**(8), 3379 (1973).
[19]G. Gerra, A. Tagantsev, N. Setter, and K. Parlinski, Phys. Rev. Lett. **96**(10), 107603 (2006).
[20]N. Pertsev, A. Zembilgotov, and A. Tagantsev, Phys. Rev. Lett. **80**(9), 1988 (1998).
[21]D. D. Fong, G. B. Stephenson, S. K. Streiffer, J. A. Eastman, O. Auciello, P. H. Fuoss, and C. Thompson, Science **304**(5677), 1650 (2004).
[22]N. A. Pertsev and H. Kohlstedt, Phys. Rev. Lett. **98**(25), 257603 (2007).
[23]A. Tagantsev, G. Gerra, and N. Setter, Phys. Rev. B **77**(17), 174111 (2008).
[24]C. Woo and Y. Zheng, Appl. Phys. A: Mater. Sci. Process. **91**(1), 59 (2008).
[25]Y. Zheng, M. Cai, and C. Woo, Acta Mater. **58**(8), 3050 (2010).
[26]D. Kim, J. Jo, Y. Kim, Y. Chang, J. Lee, J. G. Yoon, T. Song, and T. Noh, Phys. Rev. Lett. **95**(23), 237602 (2005).
[27]A. Roytburd, S. Alpay, V. Nagarajan, C. Ganpule, S. Aggarwal, E. Williams, and R. Ramesh, Phys. Rev. Lett. **85**(1), 190 (2000).
[28]L. Chen, V. Nagarajan, R. Ramesh, and A. Roytburd, J. Appl. Phys. **94**, 5147 (2003).
[29]X. Lu and H. Li, J. Appl. Phys. **109**(7), 074112 (2011).
[30]X. Lu, W. Cao, W. Jiang, and H. Li, J. Appl. Phys. **111**, 014103 (2012).